LJMU Research Online

Li, H, Liu, J, Yang, Z, Liu, RW, Wu, K and Wan, Y

 Adaptively constrained dynamic time warping for time series classification and clustering

http://researchonline.ljmu.ac.uk/id/eprint/13159/

Article

For more information please contact researchonline@ljmu.ac.uk

Adaptively constrained dynamic time warping for time series classification and clustering

Huanhuan Li [a,b,c], Jingxian Liu [a,b], Zaili Yang [c*], Ryan Wen Liu [a,b*], Kefeng Wu [d], Yuan Wan [e]

[a] Hubei Key Laboratory of Inland Shipping Technology, School of Navigation, Wuhan University of Technology, Wuhan 430063, P. R. China
[b] National Engineering Research Center for Water Transport Safety, Wuhan 430063, P. R. China
[c] Liverpool Logistics, Offshore and Marine Research Institute, Liverpool John Moores University, Liverpool L3 3AF, UK
[d] Beijing Electro-mechanical Engineering Institute, Beijing 100074, P. R. China
[e] School of Science, Wuhan University of Technology, Wuhan 430070, P. R. China
*Corresponding author.
E-mail address: Z.Yang@ljmu.ac.uk; wenliu@whut.edu.cn.

Abstract: Time series classification and clustering are important for data mining research, which is conducive to recognizing movement patterns, finding customary routes, and detecting abnormal trajectories in transport (e.g. road and maritime) traffic. The dynamic time warping (DTW) algorithm is a classical distance measurement method for time series analysis. However, the over-stretching and over-compression problems are typical drawbacks of using DTW to measure distances. To address these drawbacks, an adaptive constrained DTW (ACDTW) algorithm is developed to calculate the distances between trajectories more accurately by introducing new adaptive penalty functions. Two different penalties are proposed to effectively and automatically adapt to the situations in which multiple points in one time series correspond to a single point in another time series. The novel ACDTW algorithm can adaptively adjust the correspondence between two trajectories and obtain greater accuracy between different trajectories. Numerous experiments on classification and clustering are undertaken using the UCR time series archive and real vessel trajectories. The classification results demonstrate that the ACDTW algorithm performs better than four state-of-the-art algorithms on the UCR time series archive. Furthermore, the clustering results reveal that the ACDTW algorithm has the best performance among three existing algorithms in modeling maritime traffic vessel trajectory.

Keywords: Dynamic time warping, Distance measure, Time series classification, Vessel trajectory clustering.

1. Introduction

1.1 Background and related work

With the explosion of the Internet of Things (IoT), sensor networks and radar systems, a large number of time series are continuously produced in various fields, such as intelligent transportation, maritime engineering, clinical medicine, biological science, climate research, and social science [20, 44]. Different types of time series have been created and applied in the studies relating to hurricanes, animals, people, vessels, vehicles, and speech signals, etc [37]. Time series data mining can uncover hidden patterns and extract behavior characteristics. Time series classification and clustering are important for data mining of moving object trajectories [1, 50].

As an important kind of complex data, the time series of moving vessels play an indispensable role in maritime traffic networks, surveillance, and security research fields [22]. In the maritime traffic domain, the results of time series classification and clustering are conducive to investigating path planning[25], abnormal detection [7], and movement pattern recognition [38]. The automatic identification system (AIS) provides real-time spatiotemporal information of vessels, including time, position, speed over ground, course over ground, and rate of turn, etc. AIS is complementary to radar systems, and the temporal resolution of the AIS signal is commonly enhanced through marine radar by data fusion technology, allowing vessel trajectories to be tagged with useful information [45]. AIS systems have been widely used on vessels to identify targets and enhance maritime surveillance based on a very high frequency (VHF) data communication scheme, especially for large

cooperating vessels [2]. Trajectory classification aims at identifying features and patterns by analyzing the objects' movement awareness and other spatiotemporal information in a time series [31]. AIS-based vessel trajectory clustering is of significance in mining customary routes, identifying abnormal patterns, improving navigational safety, and safeguarding maritime surveillance and security [21]. The different types of time series are displayed in Fig. 1. Fig. 1 (a) shows vessel trajectories based on AIS data. The Gun_Point data, one of the UCR time series datasets, are presented in Fig. 1 (b). The green and blue trajectories are randomly selected from the Gun_Point data, and their corresponding relationships will be analyzed and compared in subsequent experiments.
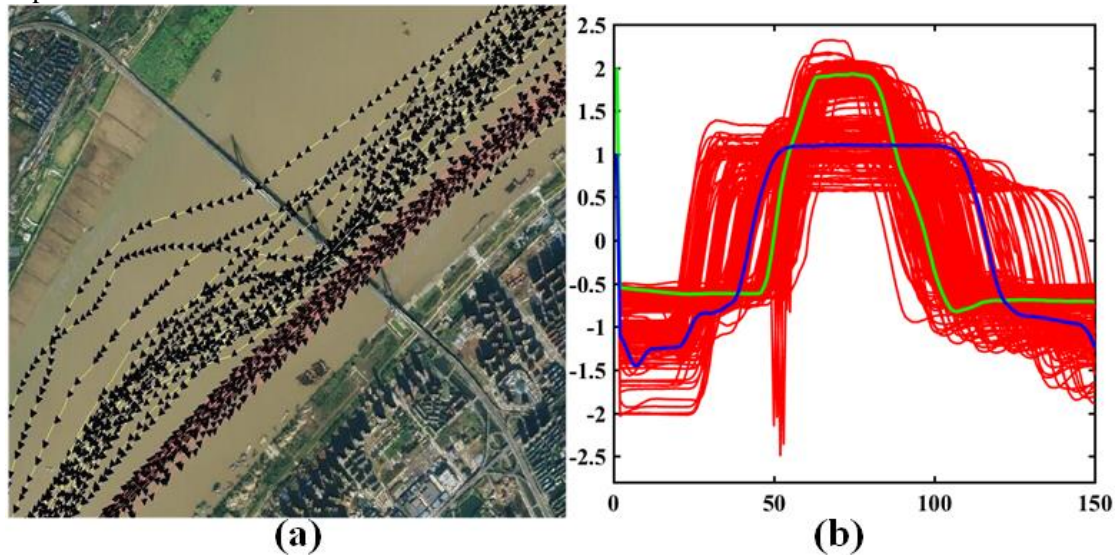

Fig.1. Different types of time series datasets: (a) AIS-based vessel trajectories, (b) one of the UCR time series datasets (Gun_Point data).

Trajectory classification [19] and clustering [13, 14] are systematic processes that include trajectory preprocessing, feature extraction, distance measurement, and grouping with and without supervision [43]. The goal of trajectory classification is to classify trajectories into predetermined classes. The classification criterion is based on the distances between trajectories. Trajectory clustering divides the trajectories into different clusters according to the distance criterion so that the within-cluster similarity of objects is as large as possible, while the between-cluster similarity is as small as possible [23]. The most basic task of trajectory classification and clustering is to measure the similarity of different trajectories. Useful distance measurement algorithms are the key to subsequent applications.

Each trajectory is composed of a large number of points. The trajectory similarity measurement method can calculate the distances between different trajectories. It is also an important factor in determining the accuracy of trajectory classification and clustering. Many advanced methods have been proposed to measure the distances between different points [3]. Previous studies have proposed popular distance measurement methods [26], such as the Euclidean distance (ED), the Hausdorff distance, the hidden Markov model (HMM), dynamic time warping (DTW), and the longest common subsequence (LCSS). The length of all trajectories must be equal in ED, which also cannot warp the time information. The Hausdorff distance has no requirement for trajectory length. The HMM distance assigns each trajectory a statistical model. However, the Hausdorff distance and HMM are time-consuming. Another criticism is that both Hausdorff and HMM have poor performance [28]. Compared with location similarity, LCSS focuses more on shape similarity and has a high time cost. It is easier for DTW to find the shape similarity between trajectories, and it also warps the routes from feature to feature. Therefore, DTW is selected as the key similarity measurement method to improve and develop in this work.

DTW was initially introduced by Velichko, Zogaruyko [39] and Itakura [16] based on dynamic programming to investigate speech recognition. Berndt and Clifford [6] proposed a detection algorithm based on DTW to find patterns in time series regarding knowledge discovery. Herbst and Coetzer [15] investigated offline handwritten signatures based on DTW. In [41], Yoshimural and Yoshimura combined DTW with the preprocessing method to verify the offline signature and

identify suspect signatures. In [34], Shanker and Rajagopalan proposed the DTW-based method to construct an effective offline signature verification system. The code-vectors and DTW are merged into the online signature verification strategy in [35] to improve the accuracy of the system. In [25], Liu *et al*. measured the similarity between trajectories and calculated the distance based on DTW to cluster the vessel trajectories and mine customary routes. In [21], Li *et al*. considered the distances between trajectories based on DTW and proposed the multistep clustering method to cluster vessel trajectories and detect abnormal trajectories. In [48], Zhao *et al*. combined DTW and the trajectory shape to analyze the distances between trajectories and mine trajectory movement patterns.

These studies have shown that DTW is a kind of nonlinear programming technique based on time programming and distance testing [30]. It can be used to calculate the similarity between two time series and eventually find the shortest distance [9]. DTW can find the optimal path with a minimum cost based on dynamic programming. However, the warped routes will also lead to over-stretching and over-compression. For example, Fig. 2 shows the pathological corresponding result obtained by DTW, where the red and blue trajectories are selected from electrocardiogram (ECG) data.
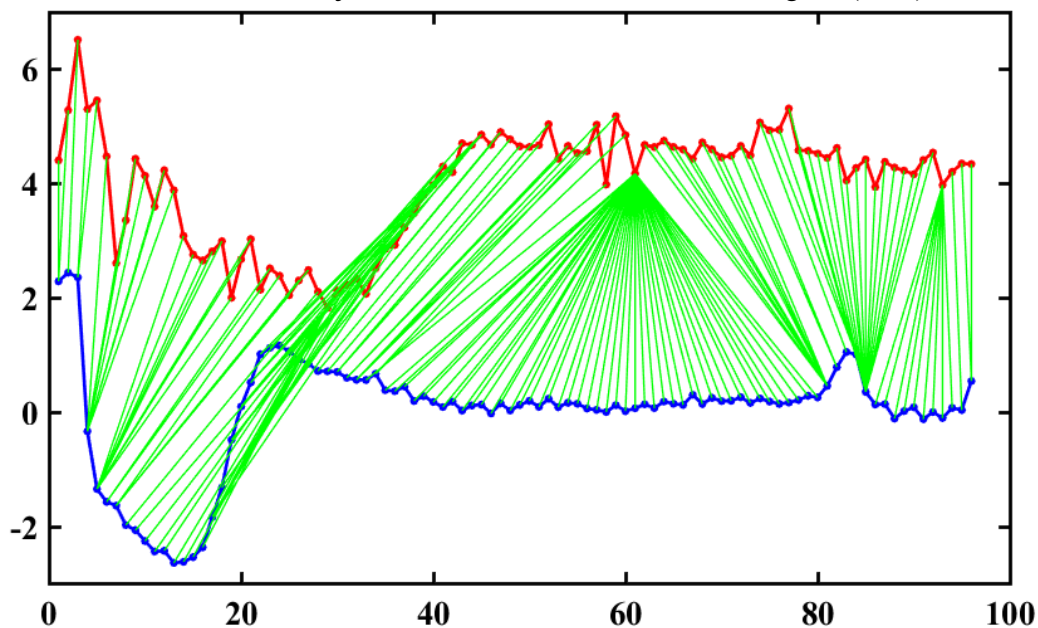

Fig.2. The pathological corresponding result obtained by DTW.

Facilitated by intensive studies of time series processing, classification, and clustering, many improved DTW algorithms have been proposed to cope with the disadvantages of off-the-shelf applications. In recent years, similarity measurement methods have attracted increasing attention in the fields of data mining and pattern recognition [47]. To date, existing DTW algorithms have mainly been improved from two perspectives: different global and local warping windows (different functions and shapes) and the selection of parameters. The global constraints are the different shapes of the warping window, such as diamond-shaped [16] and parallel regions [32]. The local constraints present a small part of the global constraints. In [32], Sakoe *et al*. proposed the slope constraint for DTW, which restricted the step size and direction of the optimal warping path. However, the continuity of the optimal path may not be guaranteed. Niennattrakul *et al*. [29] introduced an adaptive window restriction method to determine the limited optimum warping path. However, it also misses the correct warping distances. The selection of the parameter also presents a difficult problem. The derivative dynamic time warping (DDTW) algorithm was introduced in [18] to find a new path, which extracted shape information based on the derivative of the original trajectory, but the computational complexity also increased accordingly. In [40], Wan *et al*. proposed an automatic cost dynamic time warping (AC-DTW) algorithm to calculate the cost automatically and avoid over-stretching and over-compression. However, the penalty function needs to be set artificially in advance, and it is difficult to define the parameters. The weighted dynamic time warping (WDTW) and weighted DDTW (WDDTW) algorithms were developed in [17] to penalize those paths with higher phase differences based on the phase difference between test points and reference ones, then to avoid distortion of the minimum distance. However, it remains unclear how to determine the weight, and a solution needs to be found. In [4], Barbon *et al*. introduced optimized DTW based on

the discrete wavelet transform (DWT) to handle long single sequences and avoid the high computational cost. Fast dynamic time warping (FastDTW), an approximate DTW, was introduced in [33], which refined the optimal results based on a multilevel approach with linear time and space complexity. A novel time alignment measurement was proposed in [11], which could better characterize the signals. The temporal similarity information was extracted by comparing fractions of the time distortion. Novel elastic distances were proposed to further measure the amplitude difference in [24]. In [27], Morel *et al.* introduced a new tolerance to the calculation process and extended the measurement to an area of more than two time series based on DTW barycenter averaging (DBA) and constrained dynamic time warping (CDTW). In [48], Zhao *et al.* considered the combination of shape and character in the local trajectory to calculate the distance based on the original DTW and the compensation coefficient. However, the proposed method does not fundamentally improve the DTW algorithm, and different vessel trajectory characteristics cannot be measured uniformly. In [49], Zhao *et al.* developed the DTW method based on Douglas-Peucker compression and conducted clustering analysis based on the improved density-based spatial clustering of applications with noise (DBSCAN). However, this improvement cannot reduce some points based on the compression algorithm unless the algorithm is changed or the many-to-one and one-to-many problems are solved.

1.2 Motivation and contribution

The traditional DTW algorithm [6, 15, 34, 41, 42, 46] usually ignores extreme cases such as many-to-one and one-to-many when the numbers of points in different time series are extremely different. It also ignores the number of times that each point is used in the time series similarity measurement. Additionally, it does not take into account the fact that the number of points between two trajectories can vary significantly in different application aspects. Many improved DTW algorithms [4, 27, 29, 32, 40, 48] lack a unified standard and solution for the warping window shape, weight, and step size. In addition, some improved DTW algorithms also require manually preselected parameters. Extreme cases still exist in many improved DTW algorithms. To facilitate comparison with other algorithms, all the improved DTW algorithms are validated on the widely-used UCR time series with equal length. However, the pathological matching of time series is generally not considered in the mentioned warping algorithms. To address the potential limitations in traditional DTW algorithms, this paper proposes an adaptive constrained dynamic time warping (ACDTW) algorithm by considering adaptive penalty functions. In particular, ACDTW has the capacity to alleviate pathological matching and increase the accuracy of similarity measurement. Furthermore, it is not necessary to consider the window size and preselect the manual parameters for ACDTW in practical applications. Two kinds of adaptive penalty functions for time series are proposed in ACDTW: one for time series with equal length and the other for time series with unequal length. Each kind of adaptive penalty function consists of two parts: the length of the trajectory and the number of times that each point in the time series is used in each step. The proposed ACDTW can automatically adjust the correspondence of the time series, select the optimal matching, and increase the accuracy of the similarity measurement between different time series.

Given the state-of-the-art studies, the major contributions presented in this work are summarized as follows:

• To effectively handle extreme cases, the ACDTW algorithm is proposed to accurately calculate the distances between different time series. It can essentially reduce over-stretching and over-compression while improving the accuracy of distance calculation.

• The adaptive penalty functions can automatically adjust the correspondence of the time series and warp the optimal matching in each step of ACDTW. They can reduce the distance between time series with high similarity and increase the accuracy of subsequent experiments.

• Comprehensive experiments have been implemented on the UCR time series archive with equal length and realistic vessel trajectory dataset with unequal length. The results of time series classification and clustering have demonstrated the effectiveness of our ACDTW.

Automatic and valid penalty functions in the warping process can help make adjustments and find the optimal path. In this paper, the ACDTW algorithm is proposed to calculate accurate distances and reduce over-stretching and over-compression based on the penalty function of each point. The greater the similarity between two time series, the smaller the distance. ACDTW can reduce the distance between time series with high similarity while increasing the distance between time series

with low similarity. The novel penalty function can set the weight of each step automatically to select the optimal warping path. Based on the automatic warping of the novel penalty function, ACDTW can avoid many-to-one and one-to-many matching when calculating the distance and finding the optimal path between two trajectories. It enables an improvement in the accuracy of measuring trajectory distances, which can help preserve effective features, mine trajectory patterns, and support decision making effectively through trajectory classification and clustering.

The remainder of this paper is organized as follows. Section 2 briefly reviews the original DTW algorithm. In Section 3, the ACDTW algorithm is proposed and described systematically to analyze time series. In Section 4, numerous experiments are conducted based on 22 datasets from the UCR time series archive and a vessel trajectory dataset by classification and clustering respectively, to demonstrate the effectiveness of our method in practical applications. Finally, Section 5 concludes this paper by summarizing its novel contributions and future research directions.

2. A brief review of DTW

From a statistical point of view, a spatiotemporal AIS trajectory is essentially a kind of time series. Suppose $Q=\{q_1,q_2,\cdots,q_m\}$ and $C=\{c_1,c_2,\cdots,c_n\}$ denote two AIS trajectories (i.e., time series), q_i represents the value of the ith point in series Q, c_j indicates the value of the jth point in series C, m and n represent the length of the two sequences, respectively. $d(q_i,c_j)$ denotes the distance between q_i and c_j, $i = 2,3,\cdots,m, j = 2,3,\cdots n$.

DTW is used to calculate the maximum similarity between the two time series [12]. The principle of DTW is as follows:

Allocate all points in sequence according to time and then construct the matrix $A_{m\times n}$, in which $a_{ij} = d(q_i,c_j) = \sqrt{(q_i - c_j)^2} \in A_{m\times n}$. A set of adjacent matrix elements in $A_{m\times n}$ is called the warping path, denoted by $W = \{w_1,w_2,\cdots,w_t,\cdots,w_K\}$; $\max\{m,n\} < K \le m+n-1$, and the tth point in W is represented by $w_t = (a_{ij})_t$.

The warping path must satisfy the following constraints:

(1) Boundary condition: $w_1 = a_{11}, w_K = a_{mn}$;

(2) Continuity and monotonicity: if $w_{t-1} = a_{i'j'}, w_t = a_{ij}$, then $0 \le i - i' \le 1, 0 \le j - j' \le 1$, which ensures that every coordinate in the two trajectories can appear in W, and the corresponding of points between the trajectories does not intersect. The time at each point is also monotonic in W.

Specifically, DTW can be calculated as follows:

$$w_t = d(q_i,c_j)$$
$$DTW(Q,C) = \min\{\sum_{t=1}^{K} w_t / K\} \tag{1}$$

where w_t is the distance between the corresponding points q_i and c_j in the two series, and K is the length of the longer sequence.

The steps involved in the algorithm are as follows [36]:

Step 1. Calculate the DTW distance $D(i, j)$ between the two sequences from the starting points i and j of the two sequences.

$$\begin{cases} D(1,1) = d_{11} \\ D(i,j) = d_{ij} + \min\{D(i-1,j-1), D(i,j-1), D(i-1,j)\} \end{cases}$$

$$d_{ij} = d(q_i, c_j) = \sqrt{(q_i - c_j)^2} \in D_{m \times n}$$

(2)

Step 2. The distance $D(i,j)$ of the endpoint in the two sequences is the DTW distance of the two sequences.

The pseudocode of the DTW algorithm is as follows.

Algorithm 1: DTW algorithm

Input: $Q=\{q_1,q_2,\cdots,q_m\}$ and $C=\{c_1,c_2,\cdots,c_n\}$ // the two time series
Output: The optimal warping path;
       The distance of Q and C.

Initialize: $DTW(1,1) = d_{1,1}$
for i=1:n
  for j=1:m
      $D1 = d_{i,j} + DTW(i-1,j)$
      $D2 = d_{i,j} + DTW(i-1,j-1)$
      $D3 = d_{i,j} + DTW(i,j-1)$

      $DTW = \min(D1, D2, D3)$;
      The optimal path$_{i,j}$=min_index((*i*-1, *j*), (*i*-1, *j*-1), (*i*, *j*-1))
  end
end

The time complexity of ED and DTW is $O(n)$ and $O(mn)$, respectively. The optimal paths of isometric and nonisometric trajectory-based ED and DTW are shown in Fig. 3. The two green paths are the ED between the isometric and nonisometric trajectories, which show that the ED is invalid in nonisometric trajectory similarity measurements. The two red paths in Fig. 3 represent the DTW distance between the trajectories. DTW does not require that the two sequences are equal, but ED does. As shown in Fig. 3, ED cannot measure the distance between unequal trajectories.
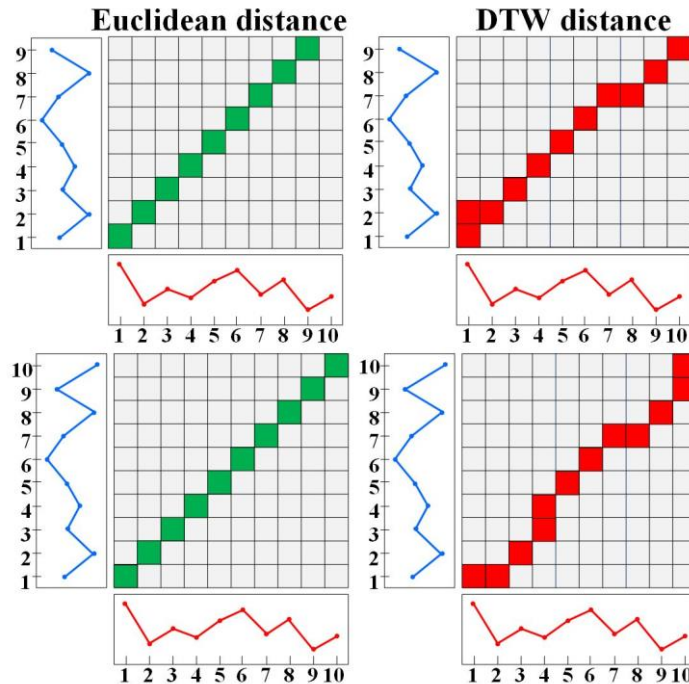

Fig.3. The optimal paths of isometric and nonisometric trajectory-based ED and DTW; the green path represents

Euclidean distance, and the red warping path expresses DTW distance.

3. The Proposed ACDTW algorithm

Penalty functions and ACDTW are introduced in this paper to reduce many-to-one and one-to-many matching. ACDTW comprehensively takes into account the use of each point, and the more times each point is used, the greater the penalty function value. The optimal warping path is selected based on the adaptive penalty functions and the number of times each point is used in each step.

3.1 The adaptive penalty functions

3.1.1 The adaptive penalty function for time series with equal length

The adaptive penalty function for time series with equal length takes into account the number of times each point is used in each step as well as the trajectories lengths. It is proposed based on the point mean idea, which does not restrict the trajectory length, as described in Eq. (3):

$$c(x_{i,j}) = [(\frac{m+n}{2})/\max(m,n)] \Box N(x_{i,j}) = \frac{m+n}{2\max(m,n)} \Box N(x_{i,j})$$

$$i = 2, \cdots, m; , j = 2, \cdots, n. \tag{3}$$

where $N(x_{i,j})$ denotes how many times each point is used in the matching process. m and n are the length of two trajectories. $\frac{m+n}{2\max(m,n)}$ is constant when m and n are defined, and it is used to numerically control the tolerance of many-to-one and one-to-many matching.

It is easy to deduce that $\frac{\min(m,n)}{\max(m,n)} \leq \frac{m+n}{2\max(m,n)} \to 1(m \to n)$, so $\frac{m+n}{2\max(m,n)}$ will increase when m and n become closer. Then, $c(x_{i,j})$ is positively proportional to $N(x_{i,j})$, meaning that when $N(x_{i,j})$ increases, $c(x_{i,j})$ increases simultaneously. A higher value of $\frac{m+n}{2\max(m,n)}$ amplifies the unacceptable degree of many-to-one and one-to-many matching, while a lower value diminishes this effect.

The value of the penalty function increases with the proximity of the two time series. This means that the closer the lengths of two time series are, the lower the tolerance of many-to-one and one-to-many matching.

3.1.2 The adaptive penalty function for time series with unequal length

The adaptive penalty function for time series with unequal length takes into account the effects of different trajectory lengths. It is enhanced based on the point mean and dual restriction ideas, as follows:

$$c(x_{i,j}) = \begin{cases} [(\frac{m+n}{2})/\max(m,n)] \Box N(x_{i,j}), 0 < \frac{m}{n} \leq \frac{1}{2} \text{ or } 0 < \frac{n}{m} \leq \frac{1}{2} \\ [\max(m,n)/(\frac{m+n}{2})] \Box N(x_{i,j}), \frac{m}{n} > \frac{1}{2} \text{ or } \frac{n}{m} > \frac{1}{2} \end{cases}$$

$$= \begin{cases} \frac{m+n}{2\max(m,n)} \Box N(x_{i,j}), 0 < \frac{m}{n} \leq \frac{1}{2} \text{ or } 0 < \frac{n}{m} \leq \frac{1}{2} \\ \frac{2\max(m,n)}{m+n} \Box N(x_{i,j}), \frac{m}{n} > \frac{1}{2} \text{ or } \frac{n}{m} > \frac{1}{2} \end{cases} \tag{4}$$

This penalty function considers the trajectory length and limits cases where the trajectory is closer

or farther. $\dfrac{2\max(m,n)}{m+n}$ and $\dfrac{m+n}{2\max(m,n)}$ are constant when m and n are defined, and they are used to numerically control the tolerance of many-to-one and one-to-many as m and n become closer or farther.

It is easy to show that $\dfrac{\min(m,n)}{\max(m,n)} \leq \dfrac{m+n}{2\max(m,n)} \to 1(m \to n) \leq \dfrac{2\max(m,n)}{m+n} < 2$, so

$\dfrac{m+n}{2\max(m,n)}$ will become larger as m and n become closer, and $\dfrac{2\max(m,n)}{m+n}$ will become larger as m and n move farther apart. A higher value of the penalty function amplifies the unacceptable degree of many-to-one and one-to-many matching.

The value of the penalty function increases with the proximity and the separation of two time series, indicating that the closer or farther the two time series are, the lower the tolerance of many-to-one and one-to-many matching.

3.2 The ACDTW algorithm

To avoid the situations of many-to-one and one-to-many matching, an adaptive penalty function is introduced into the ACDTW algorithm as the weight of each step. The proposed ACDTW algorithm is as follows:

$$ACDTW(1,1) = d_{1,1}$$

$$ACDTW(i,j) = d_{i,j} + \min \begin{cases} c(x_{i-1,j}) \square d_{i,j} + ACDTW(i-1,j) \\ ACDTW(i-1,j-1) \\ c(x_{i,j-1}) \square d_{i,j} + ACDTW(i,j-1) \end{cases} \tag{5}$$

The two matrixes $T_Q = (Q_{i,j})_{m \times n}$ and $T_C = (C_{i,j})_{m \times n}$ can constantly record the number of times each point is mapped to other points in the current path. T_Q and T_C indicate how many times each point in Q and C is used in the matching process, respectively. The optimal warping path $ACDTW(i,j)$ is found based on T_Q and T_C, where the point q_i is used $Q_{i,j}$ times and c_j is used $C_{i,j}$ times.

From Eq. (5), if the warping path is from $(i-1,j)$ to (i,j), showing that point c_j is reused, then the penalty function is added to the step for $d_{i,j}$, $Q_{i,j}=1$ and $C_{i,j}=C_{i-1,j}+1$. If the warping path is from $(i-1,j-1)$ to (i,j), showing that there is no reused point, then the penalty function will not be used in this step, $Q_{i,j}=1$ and $C_{i,j}=1$. If the warping path is from $(i,j-1)$ to (i,j), showing that point q_i is reused, then the penalty function is added to the step for $d_{i,j}$, $Q_{i,j}=Q_{i,j-1}+1$ and $C_{i,j}=1$. The ACDTW algorithm can avoid the situations of many-to-one and one-to-many matching based on the number of times each point is used in the time series.

The pseudocode of the ACDTW algorithm is summarized as follows:

Algorithm 2: ACDTW algorithm
Input: $Q=\{q_1,q_2,\cdots,q_m\}$ and $C=\{c_1,c_2,\cdots,c_n\}$ // the two time series
Output: the optimal warping path; the distance of Q and C ; The corresponding result.
Initialize: $Q_{1,1}=1, Q_{i,j}=0, i=2,\cdots,m, j=2,\cdots,n.$ $C_{1,1}=1, C_{i,j}=0, i=2,\cdots,m, j=2,\cdots,n.$ $ACDTW(1,1)=d_{1,1}$
for $i=1:n$

```
for j=1:m
    D1 = d_{i,j} + c(x_{i-1,j})□d_{i,j} + ACDTW(i-1, j)
    D2 = d_{i,j} + ACDTW(i-1, j-1)
    D3 = d_{i,j} + c(x_{i,j-1})□d_{i,j} + ACDTW(i, j-1)
    ACDTW(i, j) = min(D1, D2, D3);
    The optimal path_{i,j} = min_index((i-1, j), (i-1, j-1), (i, j-1))
    if  ACDTW(i, j) == D1
        then  Q_{i,j}=1, C_{i,j}=C_{i-1,j}+1;
            else if  ACDTW(i, j) == D2
                then  Q_{i,j}=1, C_{i,j}=1;
                    else  ACDTW(i, j) == D3
                        then  Q_{i,j}=Q_{i,j-1}+1, C_{i,j}=1.
                        Result = D (m, n)
    end
  end
end
```

4. Experimental results and analysis

DTW and its variants are proposed for matching similar time series and measuring the distances between time series. In the first classification experiment, we evaluate the classification performance of five state-of-the-art methods and demonstrate the validity of ACDTW as a distance measure on 22 benchmark datasets by the nearest neighbor classification. In the second clustering experiment, the performance of three distance measurement methods is provided and compared to further verify the accuracy and effectiveness of ACDTW on a real vessel trajectory dataset. Descriptions of the datasets, experimental setup, and performance analysis for classification and clustering are given in the following sections.

4.1. Datasets

The classification experiment is conducted on 22 datasets from the UCR time series classification archive [8, 10], which are the most widely used benchmark datasets because of their diversity. The datasets are collected from various domains and are of different types, including video data, electrocardiogram signals, images, sensor data, and synthetic data. The summary of the 22 datasets is given in Table 1, including the data type, number of classes, size of the total set, size of the training set, size of the testing set, and time series length. The number of classes and the time series length range from 1 (Fish) to 37 (Adiac) and from 60 (SyntheticControl) to 637 (Lighting2), respectively.

Table 1
Summary of datasets

Dataset	Data type	Number of classes	Size of total set	Number of training sets	Number of testing sets	Time series length
Adiac	Image	37	781	390	391	176
Beef	Spectro	5	60	30	30	470
CBF	Simulated	3	930	30	900	128
Coffee	Spectro	2	56	28	28	286
Cricket_X	Motion	12	780	390	390	300
Cricket_Y	Motion	12	780	390	390	300
Cricket_Z	Motion	12	780	390	390	300
ECG200	ECG	2	200	100	100	96
FaceAll	Image	14	2250	560	1690	131
FaceFour	Image	4	112	24	88	350

Fish	Image	1	350	175	175	463
Gun_Point	Motion	2	200	50	150	150
LargeKitchenAppliances	Device	3	750	375	375	720
Lighting2	Sensor	2	121	60	61	637
OliveOil	Spectro	4	60	30	30	570
OSULeaf	Image	6	442	200	242	427
ShapeletSim	Simulated	2	200	20	180	500
SmallKitchenAppliances	Device	3	750	375	375	720
Symbols	Image	6	1000	25	995	398
SyntheticControl	Simulated	6	600	300	300	60
Trace	Sensor	4	200	100	100	275
TwoLeadECG	ECG	2	1162	23	1139	82

The clustering experiment is implemented on the vessel trajectory dataset in the waterway around a bridge. The experimental data are collected from the AIS base station in the Wuhan section of the Yangtze River, China. The dataset relating to the bridge waterway includes the vessel trajectory data of 377 vessels involving 58,296 points. Fig. 4 shows the visualization of the vessel trajectory dataset and the length of each vessel trajectory. The trajectories come from different vessels and have different lengths.
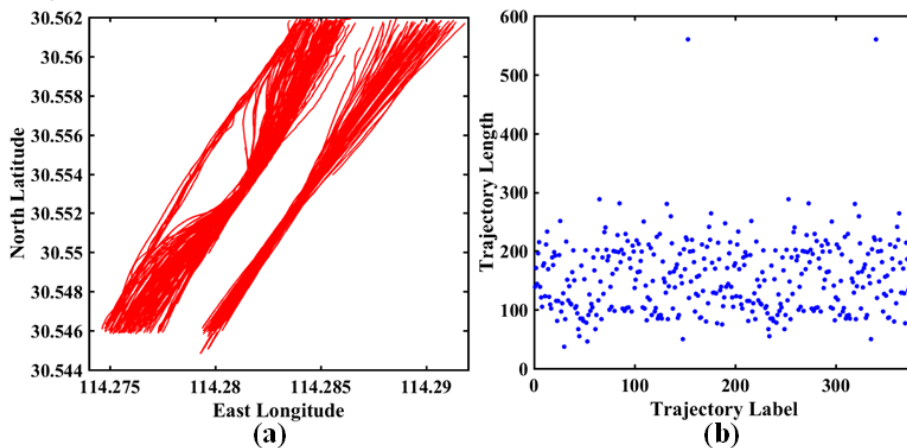

Fig.4. Visualization of the vessel trajectories and the length of each vessel trajectory.

4.2. Experimental setup

All numerical experiments are performed using 64-bit Windows 10 on a 2.60 GHz Intel Core i7-5600U CPU with 8 GB memory. The proposed ACDTW and classification algorithms are programmed in the C language, and the nearest neighbor (1NN) classifier serves as the classification standard for easy comparison with other algorithms. It is well known that 1NN has no additional parameters, and the accuracy is entirely dependent on distance. 1NN has been widely used to evaluate the performance of different similarity measurement methods [5, 10]. It is easy to use the 1NN classifier to obtain classification results based on the distances calculated by different similarity measurement algorithms. We implement a time series clustering experiment based on multiple DTW methods using MATLAB R2016a.

In this paper, the proposed ACDTW algorithm is validated by using both standard UCR time series archive and a real vessel trajectory dataset. The 22 standard datasets are chosen based on different lengths, classes, and numbers of time series from the UCR time series archive. The AIS trajectory dataset contains spatiotemporal trajectories with time, longitude, latitude, speed, etc. The 22 time series datasets are two-dimensional (2D) time series, and the AIS trajectory dataset is three-dimensional (3D) time series. The different types of time series are described and analyzed in detail in this paper to demonstrate the accuracy and robustness of the proposed ACDTW.

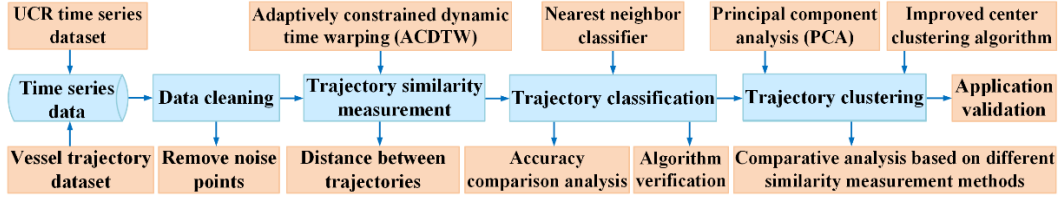The experimental flowchart is presented in Fig. 5.

Fig.5. The experimental flowchart.

4.3. Performance analysis for classification in the UCR time series archive

The classification experiment is used to verify the performance of the first adaptive penalty function. The proposed ACDTW algorithm is compared with state-of-the-art methods, which are ED, DTW, BDTW(r) (DTW of Best Warping Window), and AC-DTW(0.5). The parameter r in BDTW(r) is the percentage of the time series length. The optimal parameter 0.5 in AC-DTW(0.5) is set according to [40]. The classifiers of all algorithms are 1NN.

All the algorithms are evaluated based on the classification accuracy rate (AR) and error rate (ER) in 22 datasets, which are defined as:

$$AR = \frac{number\ of\ time\ series\ correctly\ classified}{total\ number\ of\ time\ series\ of\ test\ datasets} \qquad (6)$$

$$ER = 1 - AR$$

For easy comparison with other methods, the ER is selected as the evaluation criterion of classification performance.

4.3.1 Error rate analysis

The classification comparison results of different datasets based on different DTW algorithms are listed in Table 2. From the comparison results, we find that ED, DTW, BDTW, AC-DTW(0.5) and the new ACDTW algorithm have the best performance on 3, 4, 7, 8, and 16 of the 22 classical datasets, respectively. ACDTW significantly reduces the relevant ER, especially for Adiac, Beef, CBF, Cricket_Z, Fish, Gun_Point, and SyntheticControl. Its ERs in Adiac, Cricket_Y, ECG200, Gun_Point, LargeKitchenAppliances, OliveOil, OSULeaf, SmallKitchenAppliances, Symbols, and SyntheticControl are significantly lower than those of AC-DTW(0.5), showing a much better performance. The time axis distortion is a common situation in the time series, so DTW and its variants have better performance than ED. ED still performs better in both the ECG200 and OliveOil datasets because they have no apparent time axis distortion. The experiments compare the five algorithms, and the results show the superiority and effectiveness of the proposed ACDTW algorithm.

Table 2

1NN error rate (ER) of different measurement methods on different datasets (the best results are highlighted in bold)

Dataset	ED	DTW	BDTW(r)	AC-DTW (0.5) [40]	ACDTW
Adiac	0.3887	0.3964	0.3913(3)	0.3780	**0.3606**
Beef	0.3333	0.3667	0.3333(0)	**0.3000**	**0.3000**
CBF	0.1478	0.0033	0.0044(11)	**0.0000**	**0.0000**
Coffee	**0.0000**	**0.0000**	**0.0000(0)**	**0.0000**	**0.0000**
Cricket_X	0.4231	0.2462	0.2282(10)	**0.2102**	**0.2102**
Cricket_Y	0.4333	0.2564	0.2410(17)	0.2461	**0.2358**
Cricket_Z	0.4128	0.2462	0.2538(5)	**0.2000**	**0.2000**
ECG200	**0.1200**	0.2300	**0.1200(0)**	0.1900	0.1800
FaceAll	0.2864	0.1923	**0.1917(3)**	0.1920	0.1920
FaceFour	0.2159	0.1705	**0.1136(2)**	0.2150	0.2150
Fish	0.2171	0.1771	0.1543(4)	**0.1540**	**0.1540**
Gun_Point	0.0867	0.0933	0.0867(0)	0.0800	**0.0460**
LargeKitchenAppliances	0.5067	0.2053	0.2053(94)	0.1973	**0.1893**
Lighting2	0.2459	0.1311	0.1311(6)	**0.1147**	**0.1147**

OliveOil	**0.1333**	0.1667	**0.1333**(0)	0.1667	**0.1333**
OSULeaf	0.4793	0.4091	0.3884(7)	0.3884	**0.3842**
ShapeletSim	0.4611	0.3500	**0.3000(3)**	0.3278	0.3333
SmallKitchenAppliances	0.6587	0.3573	**0.3280(15)**	0.3573	0.3413
Symbols	0.1005	0.0503	0.0623(8)	0.0430	**0.0400**
SyntheticControl	0.1200	**0.0067**	0.0167(6)	0.0100	**0.0067**
Trace	0.2400	**0.0000**	0.0100(3)	**0.0000**	**0.0000**
TwoLeadECG	0.2529	**0.0957**	0.1317(4)	0.1281	0.1281

4.3.2 Comparison of classification accuracy

The graphical comparison results of the classification AR between ACDTW and the other four state-of-the-art algorithms are displayed in Fig. 6, and they clearly show the validity of the proposed algorithm. There are 22 points in each graph, representing the classification accuracy of ACDTW and the other methods on 22 datasets. The classification accuracy is greater than that of other methods when the points are above the line in Fig. 6. Fig. 6 (a) - (b) show that the classification accuracy of ACDTW is better than that of ED and DTW on 18 and 16 datasets respectively; Fig. 6 (c) - (d) also show the higher accuracy of ACDTW compared to that of BDTW(r) and AC-DTW(0.5) on 15 and 11 datasets, respectively.
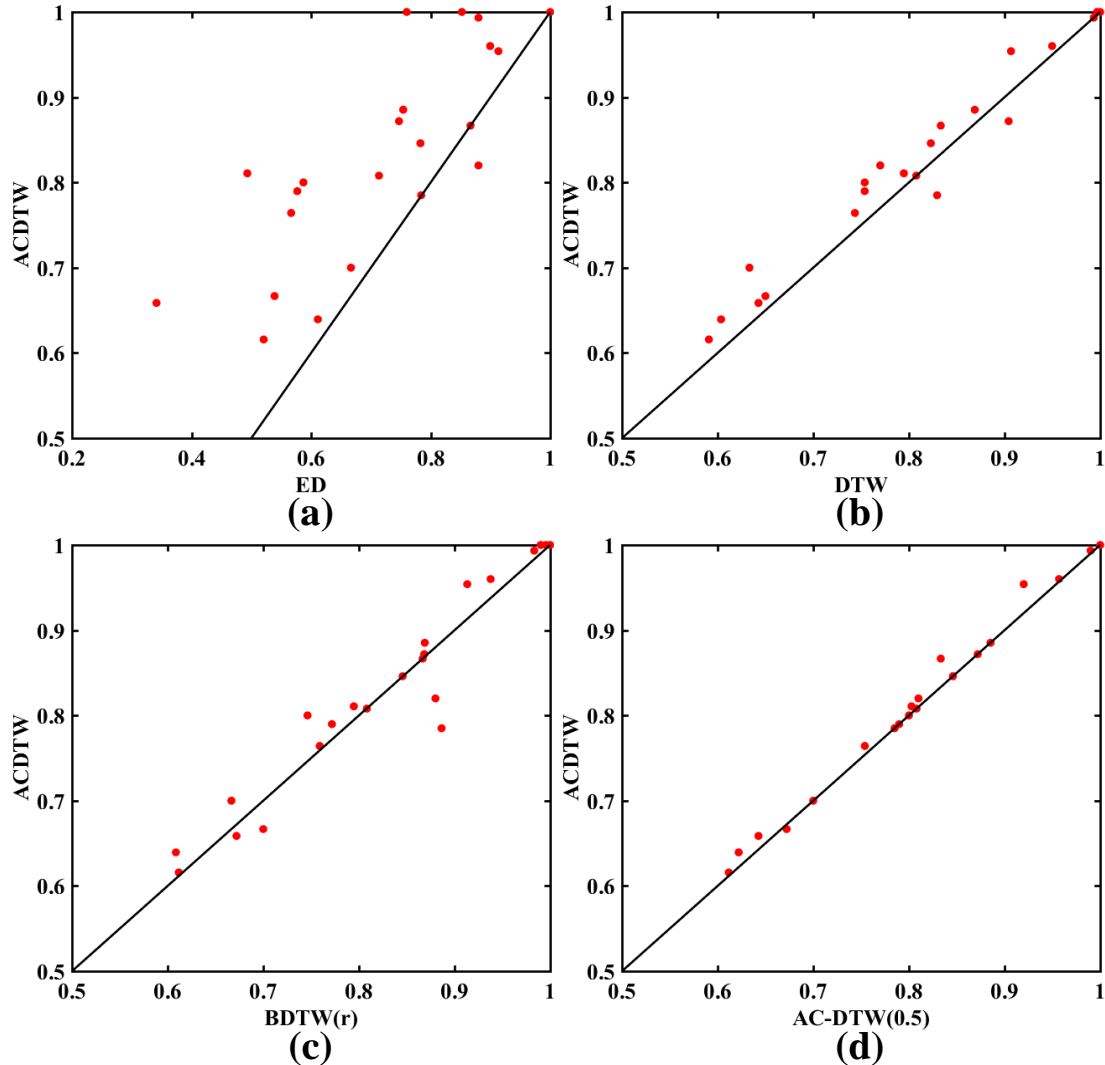

Fig.6. Comparison results of the classification accuracy of different algorithms.

To further visualize the classification AR and ER of the different algorithms, the graphical comparison results are shown in Fig. 7. The 3D histograms of AR and ER further clearly show the performance of the different algorithms. The overall trend of the proposed method ACDTW is the highest, and the ER is the lowest, in Fig. 7. The classification performance of ACDTW is the best

among the five investigated algorithms based on the comparison results and histograms in Fig. 6 and Fig. 7.
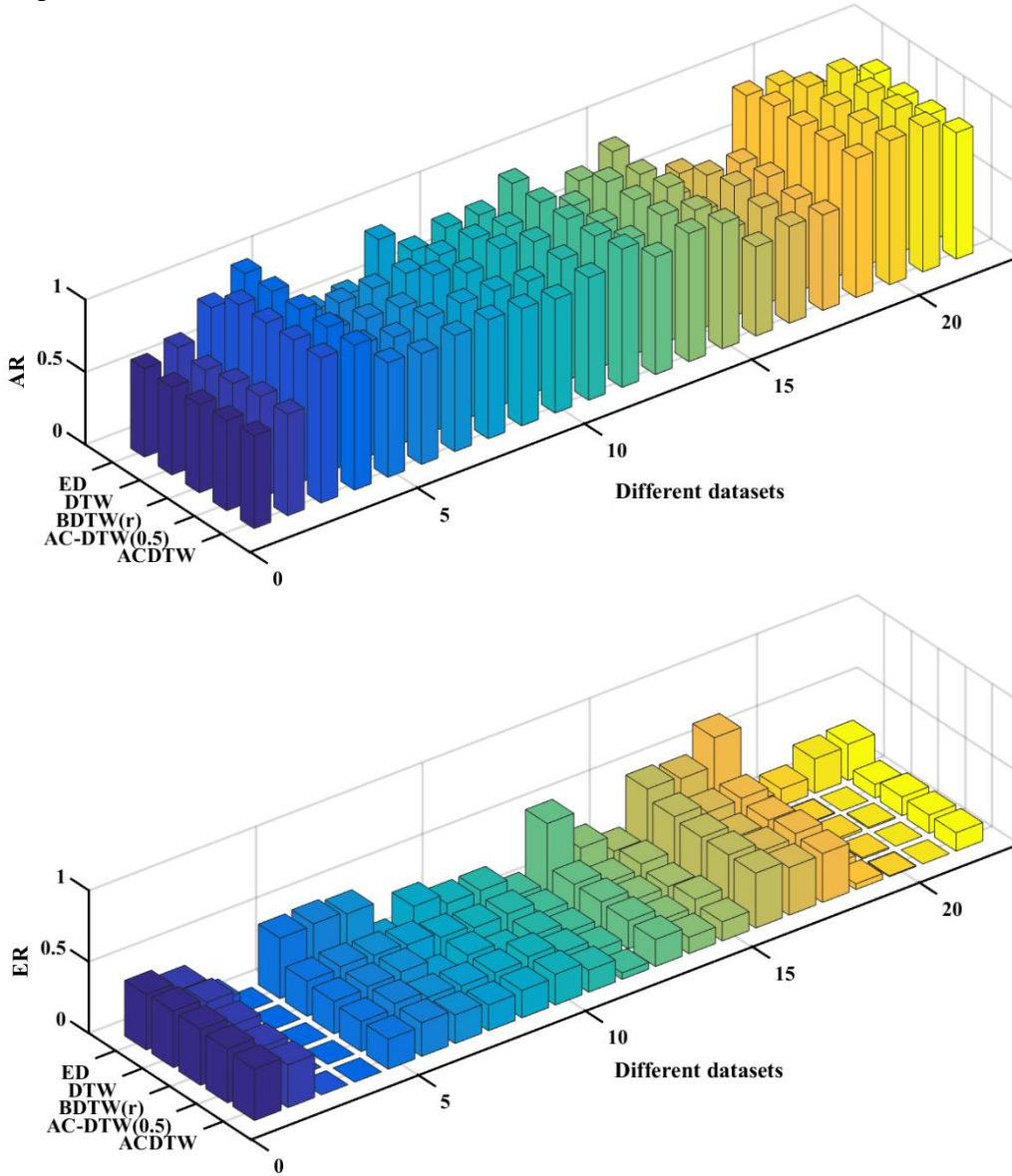

Fig.7. Graphical comparison results of the accuracy rate (AR) and error rate (ER) of the different algorithms.

4.3.3 The Texas sharpshooter fallacy

In the study of time series classification, many authors assert that their algorithm is better only because its classification accuracy is higher. This is not adequate evidence and also involves a logical error. We cannot conclude that an algorithm is more accurate on some problems unless we know in advance which datasets have higher classification accuracy (this is a subtle version of the Texas sharpshooter fallacy) [5, 46]. In further verifying the effectiveness of ACDTW, we must emphasize that ACDTW can predict in advance when ACDTW will have a higher classification accuracy. The gain is introduced here to demonstrate the performance of ACDTW, and it is given by:

$$gain = \frac{accuracy\ of\ ACDTW}{accuracy\ of\ competitor} \tag{7}$$

Leaving-one-out (LOO) cross-validation is selected to find the expected accuracy gain on the training set. An expected accuracy gain value greater than one indicates that we expect ACDTW to perform better than its competitors, and vice versa. The actual accuracy gain is calculated on the

testing set. Comparing the expected accuracy gain with the actual accuracy gain is the most effective method to verify the predictive performance of ACDTW. The results of expected accuracy gain versus actual accuracy gain between ACDTW and the competitors are shown in Fig. 8. Each point represents the result of a dataset.
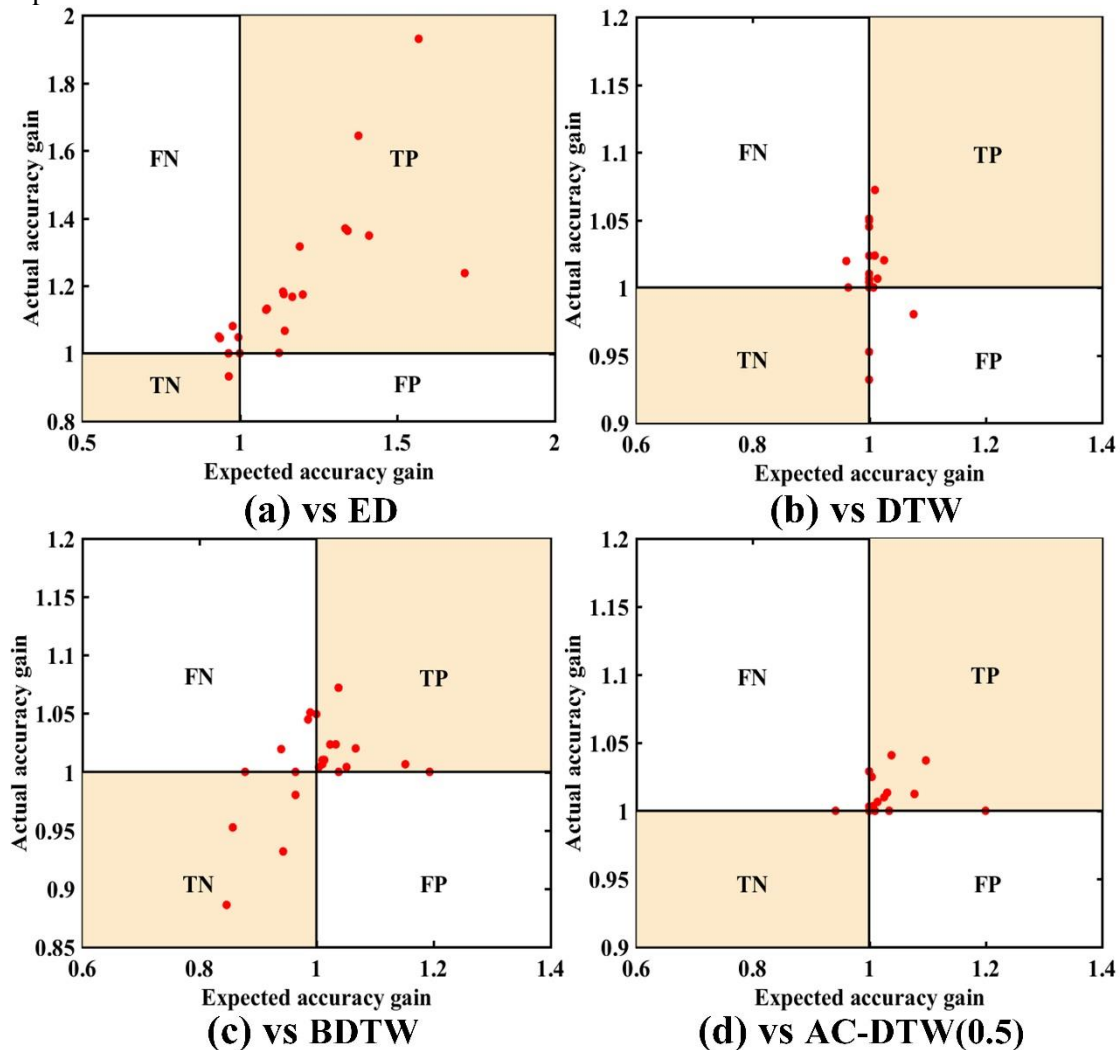

(a) vs ED

(b) vs DTW

(c) vs BDTW

(d) vs AC-DTW(0.5)

Fig. 8. Expected accuracy gain versus actual accuracy gain for the five algorithms.

As illustrated in Fig. 8, there are four cases relating to the comparison results:

TP (true positive). In this region, we predicted that ACDTW would improve classification accuracy, and this is true. Gratifyingly, the vast majority of data points fall into this region, which further demonstrates the effectiveness of ACDTW.

TN (true negative). In this region, we correctly predicted that ACDTW would decrease classification accuracy. In this case, other methods can be used to avoid the loss of accuracy.

FN (false negative). In this region, we predicted that ACDTW would decrease classification accuracy, but it improved classification accuracy.

FP (false positive). In this region, we predicted that ACDTW would improve classification accuracy, but it decreased classification accuracy. This case is the only truly bad one for us. The good result is that there is only one point falling in this region.

4.3.4 Correspondence relationship analysis

To further verify the performance of the proposed ACDTW, the correspondence relationship between two time series based on DTW, AC-DTW(0.5) and ACDTW is displayed in Fig. 9. The two time series are selected from Gun_Point data to compare and analyze the correspondence results, and the visualization of the two time series is displayed in Fig. 9(a). The original time series intersect, and the vertical distances between them are increased to display the corresponding results

more clearly. As shown in Fig. 9(b), the matching result is based on DTW, and the numbers of many-to-one and one-to-many matching situations in 9(b) are greater than those in Fig. 9(c) - (d). In the worst case, 29 points are mapped to one point. The second most extreme case is that 27 points are mapped to one point. The extreme cases mean that the two time series are severely compressed, and the features of many segments are missed in the process of matching. The matching result of AC-DTW(0.5) is shown in Fig. 9(c); the over-compression is improved, and more features are preserved. However, the numbers of many-to-one and one-to-many matching situations in Fig. 9(c) are still greater than those in Fig. 9(d), which shows the matching result of ACDTW. In Fig. 9(d), the over-compression case is significantly reduced, and the shape features are better matched and restored when using the new ACDTW algorithm. The correspondence relationship results further illustrate the validity of the proposed algorithm.
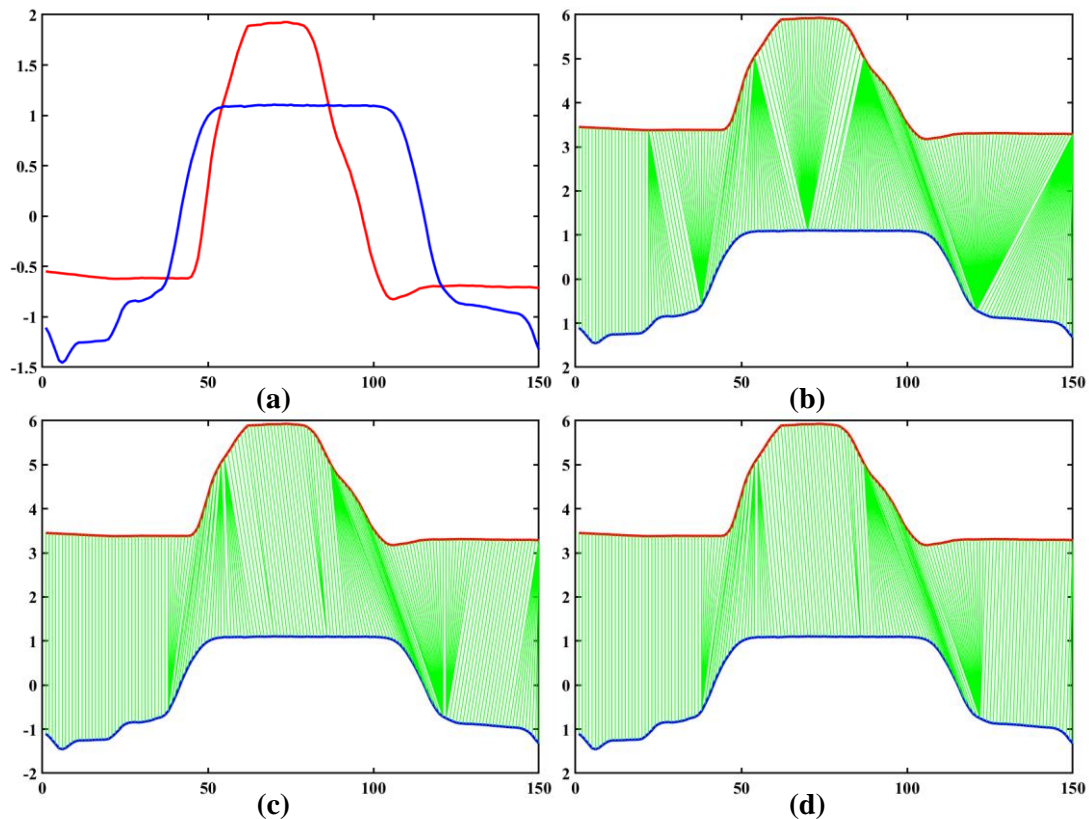

Fig. 9. The UCR time series correspondence results based on different algorithms: (a) the original trajectory in Gun_Point, (b) the result based on DTW, (c) the result based on AC-DTW(0.5), and (d) the result based on ACDTW.

4.4 Performance analysis for clustering in the vessel trajectory dataset

A clustering experiment is used to validate the performance of the second adaptive penalty function. The waterway around bridges is a high-risk area from a navigational perspective. The Yangtze River is the busiest inland waterway in the world. The vessel trajectory dataset is established based on the data collected from bridge waterways in the Wuhan section of the Yangtze River, and the relevant spatiotemporal trajectories include time, longitude, latitude, and speed.

Data cleaning is the primary step of trajectory visualization. The original trajectories are filtered by trajectory acquisition time and time intervals, and then incomplete and invalid trajectories are deleted. The original dataset includes 377 trajectories, and 324 trajectories with 51,429 points are preserved after data cleaning.

The similarity measurement of AIS trajectories by the DTW, AC-DTW(0.5) and ACDTW (with two adaptive penalty functions) are compared in this paper to further demonstrate the effectiveness and superiority of the proposed ACDTW algorithm. The first and second functions represent the adaptive penalty functions for time series with equal length and unequal length, respectively. A dimension-reduction method and the improved center clustering algorithm are introduced to cluster

the vessel trajectories. The detailed experimental process is described in [21] and is not duplicated in this paper.

4.4.1 Distance visualization based on different DTW algorithms

The distances between trajectories are calculated by different DTW algorithms. The different 324 × 324 distance matrixes are obtained by using different similarity measurement algorithms, as shown in Fig.10. The 2D image visualizations of the distance matrixes and the statistical histograms of distances based on DTW, AC-DTW(0.5), ACDTW (first function), and ACDTW (second function) are shown in Fig. 10 (a) and Fig. 10 (i), Fig. 10 (b) and Fig. 10 (j), Fig. 10 (c) and Fig. 10 (k), and Fig. 10 (d) and Fig. 10 (l). The bar charts of the distance values between the trajectories based on DTW, AC-DTW(0.5), ACDTW (first function), and ACDTW (second function) are shown in Fig. 10 (e), Fig. 10 (f), Fig. 10 (g), and Fig. 10 (h), respectively. From Fig. 10 (a) - (d), the results reveal that the distances are positively proportional to the adaptive penalty functions. The dissimilarity of trajectories is increased to facilitate data classification and clustering.

The bar charts and statistical histograms show the distribution and frequency of all the values, which are conducive to deriving features and analyzing trajectories. Trajectory clustering can group clusters based on distance.
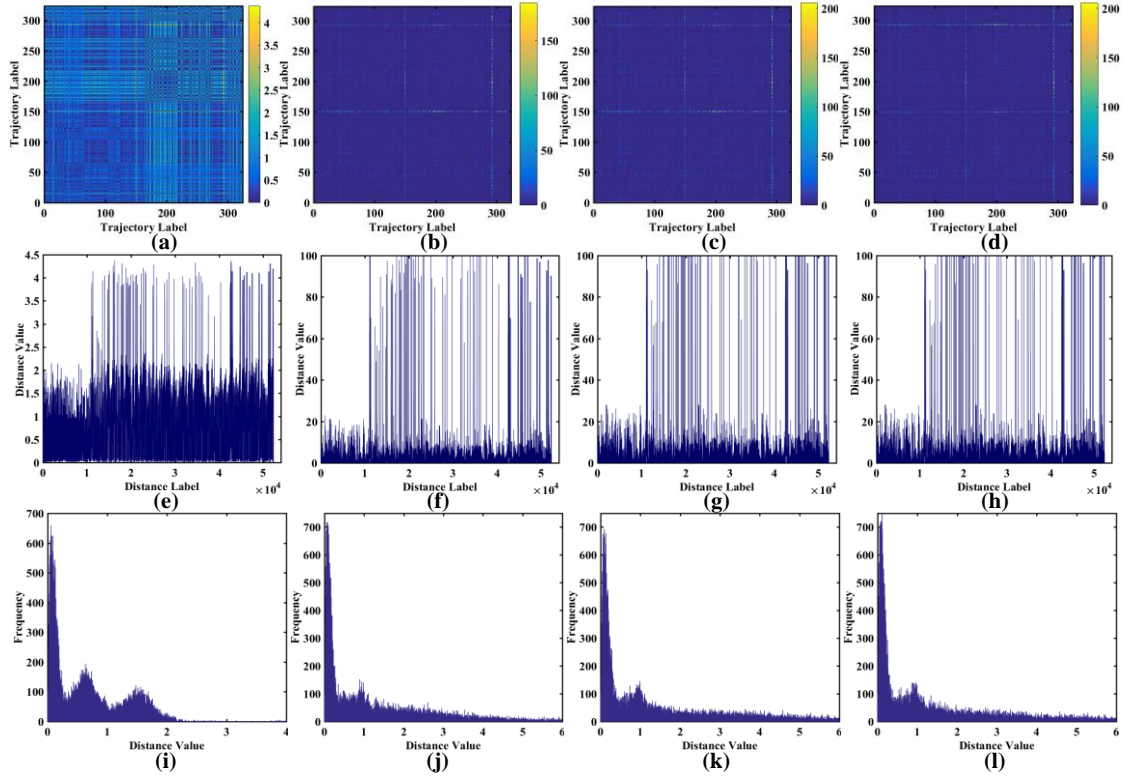

Fig. 10. Visualization of the distance matrixes obtained by different algorithms. (a) 2D image display of DTW; (b) 2D image display of AC-DTW(0.5); (c) 2D image display of ACDTW (first function); (d) 2D image display of ACDTW (second function). (e) The bar chart of all the distance values between the trajectories based on DTW; (f) the bar chart of all the distance values between the trajectories based on AC-DTW (0.5); (g) the bar chart of all the distance values between the trajectories based on ACDTW (first function); (h) the bar chart of all the distance values between the trajectories based on ACDTW (second function). (i) The statistical histogram of all the distances based on DTW; (f) the statistical histogram of all the distances based on AC-DTW (0.5); (g) the statistical histogram of all the distances based on ACDTW (first function); (h) the statistical histogram of all the distances based on ACDTW (second function).

4.4.2 Visualization of the clustering number with different DTW algorithms

To facilitate the comparison of different DTW algorithms, the clustering number is obtained by principal component analysis (PCA). The cumulative contribution rate is an important index for determining the number of cluster centers. The number of clusters k is selected according to the

cumulative contribution rate. If the cumulative contribution rate of the top k principal components is greater than 95%, then k is the number of clustering centers.

The top 10 eigenvalues and the corresponding cumulative contribution rates of the four algorithms (i.e., DTW, AC-DTW(0.5), ACDTW with the first adaptive penalty function, and ACDTW with the second adaptive penalty function) are listed in Tables 3 - 6, respectively. As shown in Table 3, the cumulative contribution rate of the top two eigenvalues is 96.99%, and that of the top three eigenvalues is 99.26%. Then, the number of clusters is set as 2. The experiments compare the clustering performance when k = 2 and k = 3 to verify the accuracy. In Table 4, the cumulative contribution rate of the top two eigenvalues based on AC-DTW(0.5) is 94.39%, and that of the top three is 96.96%. Then, we set the number of clusters to 3. The clustering performance when k = 3 and k = 4 is compared in the subsequent experiments to verify the accuracy. The cumulative contribution rates of the top ten eigenvalues based on ACDTW (first function) are shown in Table 5, and those of the top two and the top three eigenvalues are computed as 94.54% and 96.77%, respectively. Then we set the number of clusters as 3. The clustering performance when k = 3 and k = 4 is compared in the subsequent experiments to verify the accuracy. Table 6 shows the cumulative contribution rate of the top ten eigenvalues based on ACDTW (second function), and the rates of the top two and the top three eigenvalues are 94.48% and 96.71%, respectively. The number of clusters is set to 3, and the performance analysis of k = 3 and k = 4 is demonstrated in the subsequent experiments.

Table 3

The top 10 eigenvalues (EV) and the corresponding cumulative contribution rate (CCR) with PCA based on DTW.

EV	255.446	58.8111	7.35493	1.44337	0.465845	0.116907	0.112567	0.078322	0.052409	0.028119
CCR	78.84%	96.99%	99.26%	99.70%	99.85%	99.89%	99.92%	99.95%	99.96%	99.97%

Table 4

The top 10 eigenvalues (EV) and the corresponding cumulative contribution rate (CCR) with PCA based on AC-DTW(0.5).

EV	189.143	116.674	8.33211	4.45177	1.82394	0.694594	0.608764	0.432349	0.217996	0.173932
CCR	58.37%	94.39%	96.96%	98.33%	98.90%	99.11%	99.30%	99.43%	99.50%	99.55%

Table 5

The top 10 eigenvalues (EV) and the corresponding cumulative contribution rate (CCR) with PCA based on ACDTW (first penalty function).

EV	185.921	120.384	7.22493	4.77063	1.7184	0.719703	0.624671	0.497307	0.232869	0.187049
CCR	57.38%	94.54%	96.77%	98.24%	98.77%	98.99%	99.19%	99.34%	99.41%	99.47%

Table 6

The top 10 eigenvalues (EV) and the corresponding cumulative contribution rate (CCR) with PCA based on ACDTW (second penalty function).

EV	187.228	118.889	7.21503	4.8804	1.90269	0.692854	0.575127	0.494658	0.24054	0.191897
CCR	57.78%	94.48%	96.71%	98.21%	98.80%	99.01%	99.19%	99.34%	99.42%	99.48%

4.4.3 Clustering results based on different DTW algorithms

The clustering results based on different DTW algorithms are shown in Fig. 11. The performance of the four algorithms, (i.e., DTW, AC-DTW(0.5), ACDTW with the first adaptive penalty function, and ACDTW with the second adaptive penalty function) are compared and analyzed in detail. The clustering results based on DTW are shown in Fig. 11 (a) - (b), indicating poor performance on $k = 2$ and $k = 3$. Fig. 11 (c) - (d) show that the performance of clustering results based on AC-DTW(0.5) is better than that in Fig. 11 (a) - (b), showing that AC-DTW(0.5) is more effective than DTW in vessel trajectory clustering. Additionally, the clustering performance when $k = 3$ is better than that when $k = 4$, as shown in Fig. 11 (c) - (d). The red, blue and green trajectories represent different classes in Fig. 11 (c). However, it is noteworthy that 20 trajectories are misclassified. The red trajectories among the blue trajectories are misclassified. The red, blue, black, and green trajectories represent different classes in Fig. 11 (d). The red trajectories among the blue and black trajectories are misclassified.

There are many differences in the lengths of vessel trajectories, so the clustering performance based on ACDTW with two penalty functions is also compared in the experiments. The clustering results based on ACDTW with the first penalty function are shown in Fig. 11 (e) - (f), revealing better performance than DTW and AC-DTW(0.5). The clustering results show the effectiveness and reasonability of using ACDTW with the first function. Additionally, the clustering performance when $k = 3$ is better than that when $k = 4$, as shown in Fig. 11 (e) - (f). The red, blue and green trajectories represent different classes in Fig. 11 (e). The six red trajectories among the blue trajectories are misclassified. The red, blue, black, and green trajectories represent different classes in Fig. 11 (f), and the six red trajectories among the blue and black trajectories are misclassified. From Fig. 11 (g) - (h), the clustering performance based on ACDTW with the second function is better than the results of the other three algorithms. This further verifies the effectiveness and reasonability of using ACDTW with the second function. Furthermore, the clustering result when $k = 3$ is better than that when $k = 4$, as shown in Fig. 11 (g) - (h). Four trajectories are misclassified. The red, blue and green trajectories represent different classes in Fig. 11 (g). The four red trajectories among the blue trajectories are misclassified. The red, blue, black, and green trajectories represent different classes in Fig. 11 (h), and the four red trajectories among the blue and black trajectories are misclassified.

Based on the comparison and analysis in Fig. 11, the performance ranking of the four algorithms is in declining order of ACDTW with the second penalty function, ACDTW with the first penalty function, AC-DTW(0.5), and DTW.
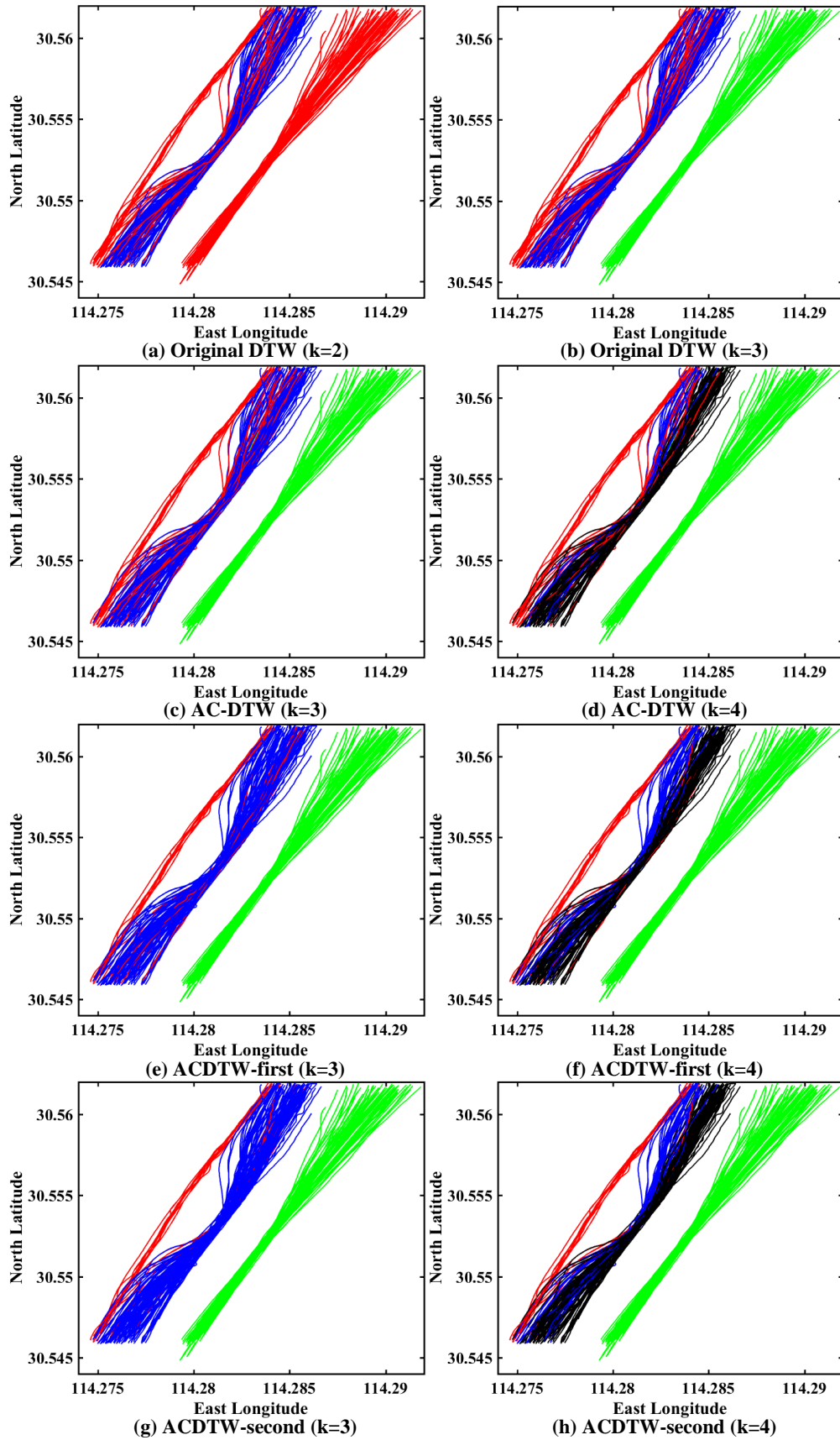
Fig. 11. Visual display of the clustering results based on different algorithms. (a) The result based on DTW (k = 2); (b) the result based on DTW (k = 3); (c) the result based on AC-DTW (k = 3); (d) the result based on AC-DTW (k = 4); (e) the result based on ACDTW with the first function (k = 3); (f) the result based on ACDTW with

4.4.4 Correspondence relationship analysis

The corresponding vessel trajectory results based on the four algorithms are clearly shown in Fig. 12. The red trajectory contains 121 points, and the blue trajectory contains 147 points. The corresponding result based on DTW is shown in Fig. 12 (a), and there are some many-to-one and one-to-many cases. Fig. 12 (b) is the corresponding result based on AC-DTW(0.5), and the extreme cases are reduced. The result based on ACDTW with the first penalty function is shown in Fig. 12 (c) and is better than those in Fig. 12 (a) and Fig. 12 (b). Fig. 12 (d), associated with ACDTW with the second penalty function, shows the best performance.
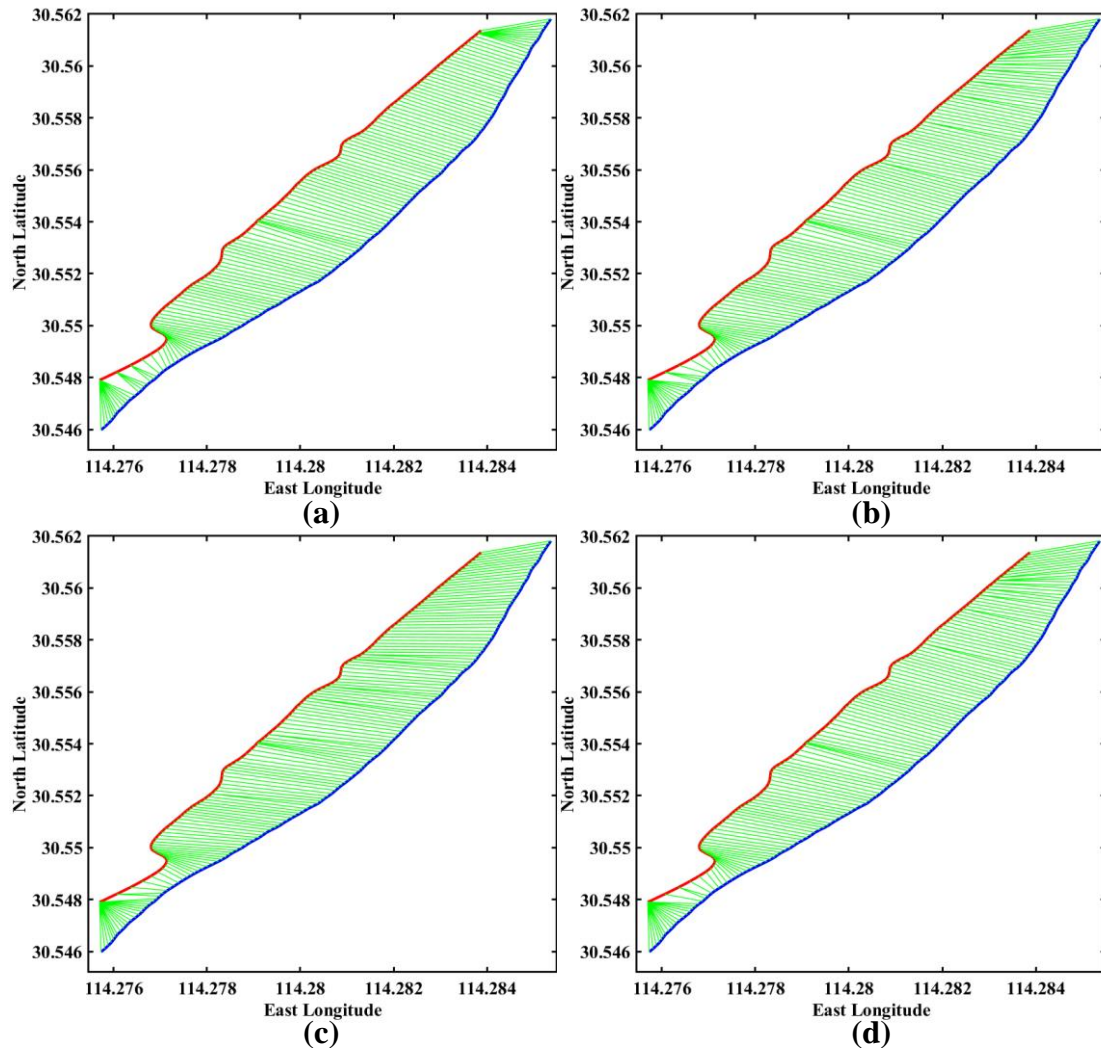

Fig. 12. The vessel trajectory correspondence results based on different algorithms, (a) DTW, (b) AC-DTW(0.5), (c) ACDTW with the first penalty function, (d) ACDTW with the second penalty function.

The corresponding vessel trajectory results with a two-fold difference in the number of points based on the four algorithms are clearly shown in Fig. 13. The corresponding result based on DTW is shown in Fig. 13 (a), and there are many-to-one cases. Between the two trajectories, each point in the red trajectory corresponds to a few points of the blue trajectory. Fig. 13 (b) is the corresponding result based on AC-DTW(0.5); the many-to-one cases are reduced and mainly allocated in the second half of the two trajectories. The corresponding result based on ACDTW with the first penalty function is shown in Fig. 13 (c), showing fewer many-to-one cases, which are allocated in the last ten points of the red trajectory. Fig. 13 (d) is the corresponding result based on ACDTW with the second penalty function; the many-to-one cases mainly appear in the last few points of the red trajectory. The dissimilarity of trajectories is increased based on the ACDTW algorithms when the difference between the numbers of points is very large.
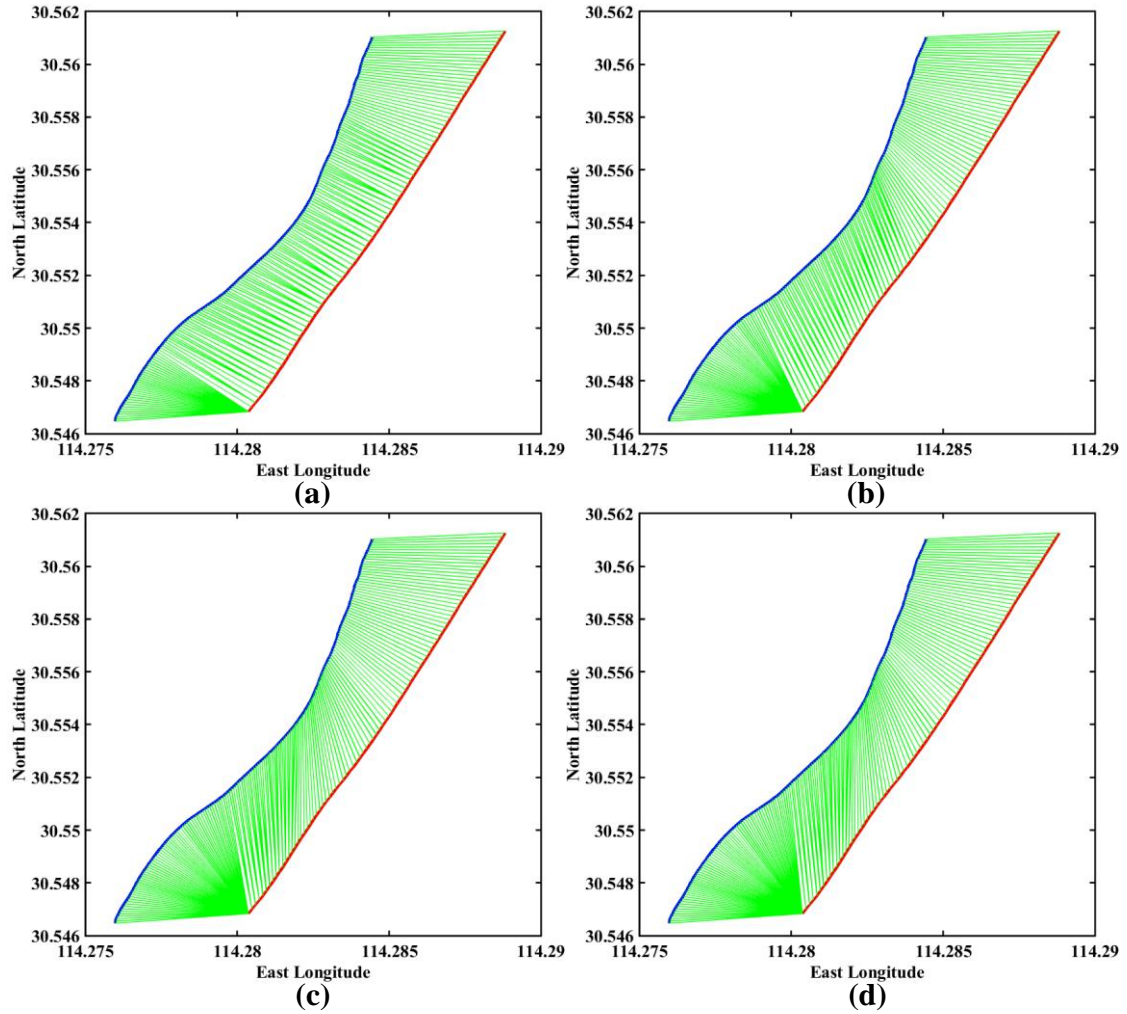
Fig. 13. The corresponding results of the vessel trajectories with a two-fold difference in the number of points based on different algorithms: (a) DTW, (b) AC-DTW(0.5), (c) ACDTW with the first penalty function, (d) ACDTW with the second penalty function.

In conclusion, the performance of the proposed ACDTW algorithm is better than that of other algorithms. The experimental results based on different types of datasets validate the effectiveness of the proposed ACDTW.

4.5 Time complexity

As DTW and ACDTW have to deal with all cells in the warping process, their time complexity is $O(mn)$, where m and n indicate the lengths of the two sequences. In addition, ACDTW considers each point in the warping matrix and records the number of times that each point is used in each step, so the time complexity of this part is also $O(mn)$. Therefore, the overall time complexity of the proposed ACDTW algorithm is $O(mn)$.

To further compare the time complexity of different algorithms, the running time (in seconds) of LOO cross-validation on the training set is displayed in Fig. 14. It shows the comparison results of the five different algorithms on six different datasets. The running time of each algorithm is consistent with its time complexity. Although ACDTW is more time-consuming than the other algorithms in five out of the six datasets, it has higher accuracy. The problem of high running time can be solved by parallel computing and other methods. It is worth noting that the proposed ACDTW can adaptively find the optimal warping path without human intervention.
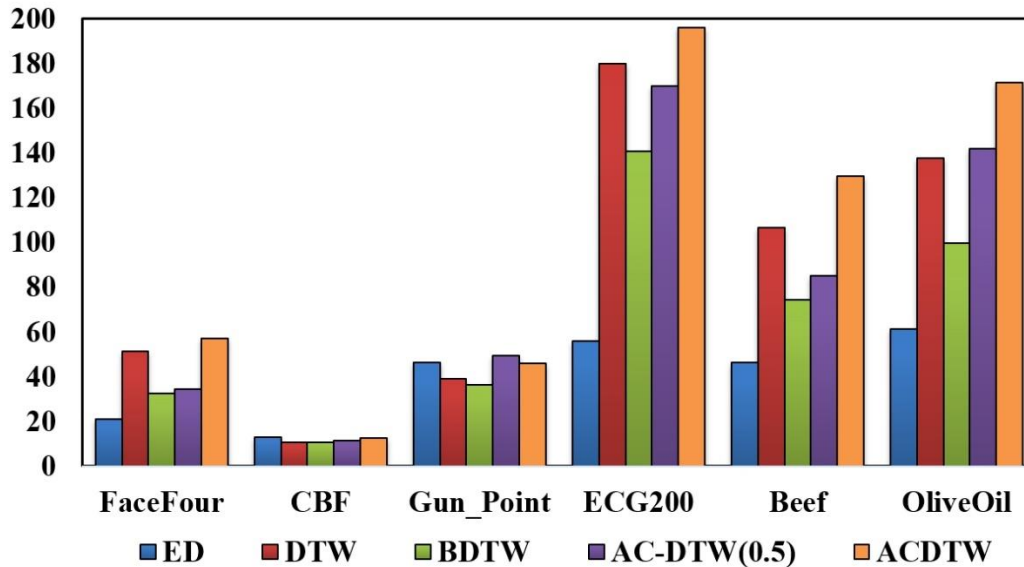
Fig.14. Running time (in seconds) of LOO cross-validation of the five different algorithms on six representative datasets

5. Conclusions

In this paper, a new algorithm, ACDTW, is proposed with the addition of two adaptive penalty functions to improve the accuracy and effectiveness of the similarity measurement between two time series. Numerous experiments based on both the UCR time series archive and vessel trajectory dataset are performed on two different time series to demonstrate the effectiveness of the ACDTW algorithm. The proposed ACDTW can provide useful solutions to the over-stretching and over-compression problems. The two penalty functions can address the long-lasting research problems of the lengths of time series, the warping path, and the number of times that each point is used. It can also capture necessary features accurately and has the best performance among the five algorithms (i.e., ED, DTW, BDTW(r), AC-DTW(0.5), and ACDTW with the two adaptive penalty functions) used for similarity measurement in the classification and clustering experiments. Valuable results such as the increased similarity between trajectories and enlarged dissimilarity are obtained from the proposed ACDTW algorithm.

To generalize the proposed ACDTW algorithm in future studies, we need to investigate how to integrate the optimal warping window and the adaptive penalty functions. In addition, the shape characteristics of the time series were introduced in [47], and we can consider the fusion of shape characteristics and the adaptive penalty functions.

Conflict of interest

The authors declare that there is no conflict of interest regarding the publication of this work.

Acknowledgment

References

[1] S. Aghabozorgi, A.S. Shirkhorshidi, T.Y. Wah, Time-series clustering–a decade review, Information Systems, 53

(2015) 16-38.

[2] R. Al-Zaidi, J.C. Woods, M. Al-Khalidi, H.S. Hu, Building novel VHF-based wireless sensor networks for the Internet of marine things, IEEE Sensors Journal, 18 (2018) 2131-2144.

[3] S. Atev, G. Miller, N.P. Papanikolopoulos, Clustering of vehicle trajectories, IEEE transactions on intelligent transportation systems, 11 (2010) 647-657.

[4] S. Barbon, R.C. Guido, L.S. Vieira, E.S. Fonseca, F.L. Sanchez, P.R. Scalassara, C.D. Maciel, J.C. Pereira, S.H. Chen, Wavelet-based dynamic time warping, Journal of Computational and Applied Mathematics, 227 (2009) 271-287.

[5] G.E. Batista, E.J. Keogh, O.M. Tataw, V.M. De Souza, CID: an efficient complexity-invariant distance for time series, Data Mining and Knowledge Discovery, 28 (2014) 634-669.

[6] D.J. Berndt, J. Clifford, Using dynamic time warping to find patterns in time series, in: Proc. of the 3rd International Conference on Knowledge Discovery and Data Mining, Seattle, WA, 1994, pp. 359-370.

[7] Y. Cai, H. Wang, X. Chen, H. Jiang, Trajectory-based anomalous behaviour detection for intelligent traffic surveillance, IET Intelligent Transport Systems, 9 (2015) 810-816.

[8] Y. Chen, E. Keogh, B. Hu, N. Begum, A. Bagnall, A. Mueen, G. Batista, The UCR time series classification archive, (2015) URL: www. cs. ucr. edu/~ eamonn/time_series_data.

[9] M.Y. Choong, R.K.Y. Chin, K.B. Yeo, K.T.K. Teo, Trajectory pattern mining via clustering based on similarity function for transportation surveillance, International Journal of Simulation-Systems, Science & Technology, 17 (2016) 19.11-19.17.

[10] H.A. Dau, A. Bagnall, K. Kamgar, C.-C.M. Yeh, Y. Zhu, S. Gharghabi, C.A. Ratanamahatana, E. Keogh, The UCR time series archive, arXiv preprint arXiv:1810.07758, (2018).

[11] D. Folgado, M. Barandas, R. Matias, R. Martins, M. Carvalho, H. Gamboa, Time alignment measurement for time series, Pattern Recognition, 81 (2018) 268-279.

[12] T. Gorecki, M. Luczak, Using derivatives in time series classification, Data Mining and Knowledge Discovery, 26 (2013) 310-331.

[13] C. Gupta, A. Jain, D.K. Tayal, O. Castillo, ClusFuDE: Forecasting low dimensional numerical data using an improved method based on automatic clustering, fuzzy relationships and differential evolution, Engineering Applications of Artificial Intelligence, 71 (2018) 175-189.

[14] Y. Han, L. Zhu, Z. Cheng, J. Li, X. Liu, Discrete optimal graph clustering, IEEE Transactions on Cybernetics,

50 (2020) 1697-1710.

[15] B. Herbst, H. Coetzer, On an offline signature verification system, in: Proc. of the 9th Annual South African Workshop on Pattern Recognition, 1998, pp. 39-43.

[16] F. Itakura, Minimum prediction residual principle applied to speech recognition, IEEE T Acoust Speech, 23 (1975) 67-72.

[17] Y.S. Jeong, M.K. Jeong, O.A. Omitaomu, Weighted dynamic time warping for time series classification, Pattern Recognition, 44 (2011) 2231-2240.

[18] E.J. Keogh, M.J. Pazzani, Derivative dynamic time warping, in: Proc. of the 2001 SIAM International Conference on Data Mining, 2001, pp. 1-11.

[19] M. Krawczak, G. Szkatuła, An approach to dimensionality reduction in time series, Information Sciences, 260 (2014) 15-36.

[20] J.S.L. Lam, K.P.B. Cullinane, P.T.-W. Lee, The 21st-century Maritime Silk Road: challenges and opportunities for transport management and practice, Transport Reviews, 38 (2018) 413-415.

[21] H. Li, J. Liu, R. Liu, N. Xiong, K. Wu, T. Kim, A dimensionality reduction-based multi-step clustering method for robust vessel trajectory analysis, Sensors, 17 (2017) 1792.

[22] H. Li, J. Liu, K. Wu, Z. Yang, R. Liu, N. Xiong, Spatio-temporal vessel trajectory clustering based on data mapping and density, IEEE Access, 6 (2018) 58939-58954.

[23] T.W. Liao, Clustering of time series data—a survey, Pattern recognition, 38 (2005) 1857-1874.

[24] J. Lines, A. Bagnall, Time series classification with ensembles of elastic distance measures, Data Mining and Knowledge Discovery, 29 (2015) 565-592.

[25] J. Liu, H. Li, Z. Yang, K. Wu, Y. Liu, R.W. Liu, Adaptive Douglas-Peucker algorithm with automatic thresholding for AIS-based vessel trajectory compression, IEEE Access, 7 (2019) 150677-150692.

[26] W.-K. Loh, S. Mane, J. Srivastava, Mining temporal patterns in popularity of web items, Information Sciences, 181 (2011) 5010-5028.

[27] M. Morel, C. Achard, R. Kulpa, S. Dubuisson, Time-series averaging using constrained dynamic time warping with tolerance, Pattern Recognition, 74 (2018) 77-89.

[28] B. Morris, M. Trivedi, Learning trajectory patterns by clustering: Experimental studies and comparative evaluation, in: 2009 IEEE Conference on Computer Vision and Pattern Recognition, Miami, FL, USA, 2009, pp.

312-319.

[29] V. Niennattrakul, C.A. Ratanamahatana, On clustering multimedia time series data using k-means and dynamic time warping, in: 2007 International Conference on Multimedia and Ubiquitous Engineering (MUE'07), Seoul, Korea, 2007, pp. 733-738.

[30] F. Petitjean, G. Forestier, G.I. Webb, A.E. Nicholson, Y.P. Chen, E. Keogh, Faster and more accurate classification of time series by exploiting a novel dynamic time warping averaging algorithm, Knowledge and Information Systems, 47 (2016) 1-26.

[31] R. Saini, P.P. Roy, D.P. Dogra, A novel point-line duality feature for trajectory classification, The Visual Computer, 35 (2019) 415-427.

[32] H. Sakoe, S. Chiba, Dynamic-programming algorithm optimization for spoken word recognition, IEEE Transactions on Acoustics Speech and Signal Processing, 26 (1978) 43-49.

[33] S. Salvador, P. Chan, Toward accurate dynamic time warping in linear time and space, Intelligent Data Analysis, 11 (2007) 561-580.

[34] A.P. Shanker, A.N. Rajagopalan, Off-line signature verification using DTW, Pattern Recognition Letters, 28 (2007) 1407-1414.

[35] A. Sharma, S. Sundaram, An enhanced contextual DTW based system for online signature verification using Vector Quantization, Pattern Recognition Letters, 84 (2016) 22-28.

[36] D.F. Silva, R. Giusti, E. Keogh, G.E.A.P.A. Batista, Speeding up similarity search under dynamic time warping by pruning unpromising alignments, Data Mining and Knowledge Discovery, 32 (2018) 988-1016.

[37] J. Soto, O. Castillo, P. Melin, W. Pedrycz, A new approach to multiple time series prediction using MIMO fuzzy aggregation models with Modular Neural Networks, International Journal of Fuzzy Systems, 21 (2019) 1629-1648.

[38] F. Tu, S.S. Ge, Y.S. Choo, C.C. Hang, Sea state identification based on vessel motion response learning via multi-layer classifiers, Ocean Engineering, 147 (2018) 318-332.

[39] V.M. Velichko, N.G. Zagoruyko, Automatic recognition of 200 words, International Journal of Man-Machine Studies, 2 (1970) 223-234.

[40] Y. Wan, X. Chen, Y. Shi, Adaptive cost dynamic time warping distance in time series analysis for classification, Journal of Computational and Applied Mathematics, 319 (2017) 514-520.

[41] M. Yoshimural, I. Yoshimura, An application of the sequential dynamic programming matching method to off-

line signature verification, in, Springer Berlin Heidelberg, Berlin, Heidelberg, 1997, pp. 299-310.

[42] C. Yu, L. Luo, L.L.-H. Chan, T. Rakthanmanon, S. Nutanong, A fast LSH-based similarity search method for multivariate time series, Information Sciences, 476 (2019) 337-356.

[43] G. Yuan, P.H. Sun, J. Zhao, D.X. Li, C.W. Wang, A review of moving object trajectory clustering algorithms, Artificial Intelligence Review, 47 (2017) 123-144.

[44] J. Zhang, H. Li, Q. Gao, H. Wang, Y. Luo, Detecting anomalies from big network traffic data using an adaptive detection approach, Information Sciences, 318 (2015) 91-110.

[45] W. Zhang, F. Goerlandt, J. Montewka, P. Kujala, A method for detecting possible near miss ship collisions from AIS data, Ocean Engineering, 107 (2015) 60-69.

[46] Z. Zhang, R. Tavenard, A. Bailly, X. Tang, P. Tang, T. Corpetti, Dynamic time warping under limited warping path length, Information Sciences, 393 (2017) 91-107.

[47] J. Zhao, L. Itti, Shapedtw: shape dynamic time warping, Pattern Recognition, 74 (2018) 171-184.

[48] L. Zhao, G. Shi, A novel similarity measure for clustering vessel trajectories based on Dynamic Time Warping, The Journal of Navigation, 72 (2019) 290-306.

[49] L. Zhao, G. Shi, A trajectory clustering method based on Douglas-Peucker compression and density for marine traffic pattern recognition, Ocean Engineering, 172 (2019) 456-467.

[50] Y. Zheng, Trajectory data mining: an overview, ACM Transactions on Intelligent Systems and Technology, 6 (2015) 1-41.